Reactions of Diarylnitrenium Ions with Electron Rich Alkenes: An Experimental and Theoretical Study

Ricardo J. Moran, Christopher Cramer,† and Daniel E. Falvey*,‡

Department of Chemistry and Supercomputer Institute, University of Minnesota, Minneapolis, Minnesota, 55455, and Department of Chemistry & Biochemistry, University of Maryland, College Park, Maryland 20742

Received December 17, 1996⊗

Photolysis of *N*-(diphenylamino)-2,4,6-trimethylpyridinium tetrafluoroborate (**1a**) and *N*-[bis(4-methylphenyl)amino]-2,4,6-trimethylpyridinium salt (**1b**) gives products attributable to diarylnitrenium ion (Ar_2N^+, **2**). The major products of these reactions include products from nucleophilic addition of various π-nucleophiles (e.g. electron rich alkenes) to the ortho and para positions of one of the phenyl rings. Nanosecond and EPR spectroscopy show that radicals also form. These radicals are thought to give rise to the diarylamines isolated as minor products from the photolysis of **1a** and **1b**. In addition to the para addition products and Ph_2NH, *N*-phenylindoles and *N*-phenylindolinones are isolated when silyl enol ethers and silyl ketene acetals are used as trapping agents, respectively. The indoles and indolinones are generated from initial addition of the nucleophile to the ortho position on **2** followed by cyclization of the resulting intermediate. A product resulting from N addition of the nucleophile to **2** is isolated only when silyl ketene acetals are used. A number of electronic sturcture calculations at different levels of molecular orbital and density functional theory were carried out on Ph_2N^+. There do not seem to be effects associated with either the charge distribution or the LUMO that would strongly influence ortho/para/N selectivity in nucleophilic trapping. Laser flash photolysis on **1a** provides absolute rate constants for the nucleophilic addition of various alkenes to Ph_2N^+. These fall in the range of 10^9-10^{10} M^{-1} s^{-1} and correlate with the oxidation potential of the alkene. From these data it is clear that the more easily oxidized the alkene the faster it will react with Ph_2N^+.

Introduction

Nitrenium ions, and more specifically aryl-substituted nitrenium ions, are reactive intermediates that have been the subject of much recent attention.[1−4] One reason for this is the proposal that arylnitrenium ions are intermediates in the reactions whereby various chemical carcinogens damage DNA.[5−9] The target of this reaction appears to be the guanine bases in the DNA molecule.[10] In the past several years laser flash photolysis techniques have been applied to the study of arylnitrenium ions.[11−14] These have confirmed that the arylnitrenium ions alleged to be involved in the carcinogenic pathways do in fact react very rapidly with the critical DNA components.[15] Moreover, it has become increasingly clear that various para-substitued phenylnitrenium ions have microsecond or longer lifetimes in water.[12]

Arylnitrenium ions are ambident electrophiles. As indicated in eq 1, there are three distinct sites where positive charge is localized: at nitrogen, at the para ring carbon, and at the ortho ring carbons. One might expect nucleophilic attack at any or all of these sites. Of course these same considerations apply to the isoelectronic carbenium ions (eq 2). In practice, however, nucleophiles

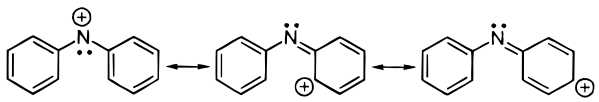

(1)

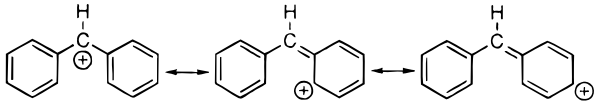

(2)

add almost exclusively to the exocyclic carbon atom of the carbenium ion.[12] In contrast, arylnitrenium ions are almost always attacked by nucleophiles at the ring carbons rather than the exocyclic nitrogen.[1,2,4] In fact an examination of the literature reveals very few bona fide examples of nucleophilic addition to nitrogen. One

* Author to whom correspondance should be addressed.
† University of Minnesota.
‡ University of Maryland.
⊗ Abstract published in *Advance ACS Abstracts,* April 1, 1997.

(1) Robbins, R. J.; Falvey, D. E. *Tetrahedron Lett.* **1994**, *35*, 4943−4946.
(2) Robbins, R. J.; Yang, L. L.-N.; Anderson, G. B.; Falvey, D. E. *J. Am. Chem. Soc.* **1995**, *117*, 6544−6552.
(3) McCelland, R. A.; Kahley, M. J.; Davidse, P. A. *J. Phys. Org. Chem.* **1996**, *9*, 355−360.
(4) Moran, R. J.; Falvey, D. E. *J. Am. Chem. Soc.* **1996**, *118*, 8965−8966.
(5) Kadlubar, F. F.; Beland, F. A. In *Polycyclic Hydrocarbons and Carcinogesis*; Harvey, R. G., Ed.; American Chemical Society: Washington, DC, 1985.
(6) Frederick, C. B.; Beland, F. A. In *Polycyclic Aromatic Hydrocarbon Carcinogenesis: Structure-Activity Relationships*; Yang, S. K., Silverman, B. D., Eds.; CRC: Boca Raton, FL, 1988; Vol. II, pp 111−139.
(7) Turesky, R. J.; Lang, N. P.; Butler, M. A.; Teitel, C. H.; Kadlubar, F. F. *Carcinogenesis* **1991**, *12*, 1839−1845.
(8) Kadlubar, F. F. In *DNA Adducts Identification and Significance*; Hemminki, K.; Dipple, A.; Shuker, D. E. G.; Kadlubar, F. F.; Segerbäck, D.; Bartsch, H., Eds.; University Press: Oxford, UK, 1994; pp 199−216.
(9) Turesky, R.; Markovic, J. *Chem. Res. Toxicol.* **1994**, *7*, 752−761.
(10) Schut, H. A. J.; Castongauy, A. *Drug Metab. Rev.* **1984**, *15*, 753−839.
(11) Anderson, G. B.; Yang, L. L.-N.; Falvey, D. E. *J. Am. Chem. Soc.* **1993**, *115*, 7254−7262.
(12) Davidse, P. A.; Kahley, M. J.; McClelland, R. A.; Novak, M. *J. Am. Chem. Soc.* **1994**, *116*, 4513−4514.
(13) McClelland, R. A.; Davidse, P. A.; Hadzialic, G. *J. Am. Chem. Soc.* **1995**, *117*, 4173−4174.
(14) McClelland, R. A.; Kahley, M. J.; Davidse, P. A.; Hadzialic, G. *J. Am. Chem. Soc.* **1996**, *118*, 4794−4803.
(15) Novak, M.; Kennedy, S. A. *J. Am. Chem. Soc.* **1995**, *117*, 574−575.

S0022-3263(96)02364-X CCC: $14.00

Scheme 1. General Photochemical Mechanism for the Photolysis of 1

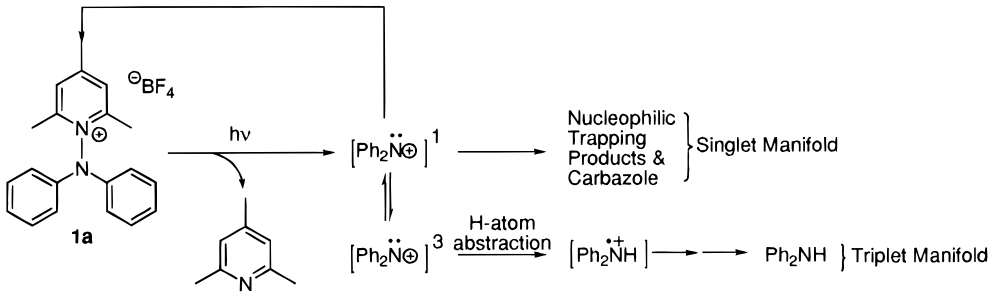

signficant exception to this is the reaction of guanosine with *N*-acylarylnitrenium ions.[15] In this case, a covalent bond is formed between the nitrogen of the nitrenium ion and the C-8 position of guanosine (eq 3). This raises an important question: Is guanosine unique in adding to nitrogen or, will any π-nucleophile add to that site?

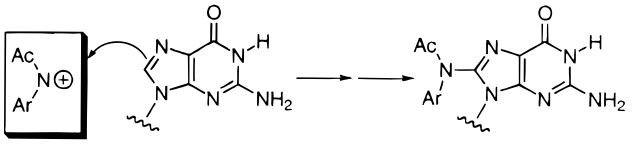

(3)

Parham and Templeton examined the regiochemistry of nucleophilic addition to purinium cations and rationalized their results in terms of a frontier molecular orbital (FMO) analysis.[16] Extension of this analysis to simple arylnitrenium ions leads to the following predictions. The *n*-nucleophiles (e.g. Cl^- and ROH) are either negatively charged or possess strong dipoles. As a consequence, they will be attracted to sites of high positive charge density. In arylnitrenium ions, this is likely to be the carbon atoms, as carbon is more electropositive than nitrogen. Guanosine, on the other hand, is a much less polar and more delocalized nucleophile. It follows that such a nucleophile would tend to add to the site of the highest LUMO coefficient. In the case of the arylnitrenium ions this site could be at the nitrogen.

Aside from the aforementioned guanosine experiments, there appear to be very few systematic studies on the reactions of arylnitrenium ions with π-nucleophiles (i.e., electron rich alkenes and electron rich arenes). Swenton et al. examined the reactions of *N*-acetyl-*N*-(*p*-alkoxyphenyl)nitrenium ions with β-methylstyrene.[17] They found that most of the products occured from addition of β-carbon of β-methylstyrene to the orthocarbon atom of the nitrenium ion. Many early nitrenium ion studies focusing on apparent N-addition showed that the nucleophile seemed to add via an S_N2 mechanism which did not involve a free nitrenium ion.[18−20]

The general objective of this study was to determine how π-nucleophiles add to simple diarylnitrenium ions and if possible to identify trends in the ratio of N-addition to C-addition products. In particular, we wanted to test whether the simple FMO picture described above is adequate to predict the regiochemical outcomes of these reactions. To this end, we examined the products and rate constants from the reactions of various alkenes with diphenylnitrenium ion. In support of these experiments, we have also carried out density functional (DFT) calculations on Ph_2N^+ in order to predict how the charges and frontier orbitals are distributed on that species. Analysis of the electronic structure of Ph_2N^+ and other arylnitrenium ions indicates that both the positive charge and the LUMO density are distributed fairly evenly among the three positions identified in the simple resonance picture. Such charge distribution and LUMO density would suggest that addition of nucleophiles would occur with near equal probability at all three sites. Our results indicate, however, that this is not the case. Most, and in some cases all, nucleophilic addition occurs at the para position. More importantly, N-addition does *not* seem to be a general property of π-nucleophiles. In fact, only very electron rich alkenes add to the nitrogen of the nitrenium ion. Even then, products resulting from nitrogen addition are isolated in relatively low yields.

Results and Discussion

We have previously communicated results from our studies on the photochemistry of 1-(*N*,*N*-diphenylamino)-trimethylpyridinium tetrafluoroborate (**1a**).[4] It was shown that the primary photochemical processes involves scission of the N−N bond leading to diphenylnitrenium ion (**2a**) (Ph_2N^+). The singlet state of the latter species was detected by laser flash photolysis (LFP). From product studies, it was found that nucleophiles such as CH_3OH and EtOH add rapidly to singlet state Ph_2N^+ only at the para position, while Cl^- adds to both the ortho and para ring carbons. In addition to the singlet state chemistry, the earlier study also identified a parallel triplet pathway that leads to the production of the diphenylamine cation radical ($Ph_2NH^{+\bullet}$). This intermediate is produced via H atom abstraction, most likely from the solvent, by the triplet nitrenium ion. Eventually, this latter pathway leads to the production of diphenylamine (Ph_2NH). These photochemical pathways are summarized in Scheme 1.

Photochemistry of 1a in the Absence of Traps. Generation of Ph_2N^+ in the absence of any trapping agents (either nucleophiles for the singlet state or H atom donors for the triplet state) provides a highly complex mixture of colored materials. Diphenylamine (Ph_2NH) and carbazole are detected in low yields. We assume that the intractable material consists of oligomers and polymers of carbazole and Ph_2NH. Both of these species are known to polymerize under oxidizing conditions.[21,22] It is likely, therefore, that carbazole and Ph_2NH are formed as primary photoproducts which are then consumed by reactions with subsequently generated Ph_2N^+ and/or $Ph_2N^{\bullet}$.

(16) Parham, J. C.; Templeton, M. A. *J. Org. Chem.* **1982**, *47*, 652−657.
(17) Dalidowicz, P.; Swenton, J. S. *J. Org. Chem.* **1993**, *58*, 4802−4804.
(18) Ohta, T.; Shudo, K.; Okamoto, T. *Tetrahedron Lett.* **1978**, *23*, 1983−1986.
(19) Novak, M.; Martin, K. A.; Heinrich, J. L. *J. Org. Chem.* **1989**, *54*, 5430−5431.
(20) Ulbrich, R.; Famulok, M.; Bosold, F.; Boche, G. *Tetrahedron Lett.* **1990**, *31*, 1689−1692.
(21) Welzel, P. *Chem. Ber.* **1970**, *103*, 1318−1333.
(22) Waltman, R. J.; Bargon, J. *Can. J. Chem.* **1986**, *64*, 76−95.

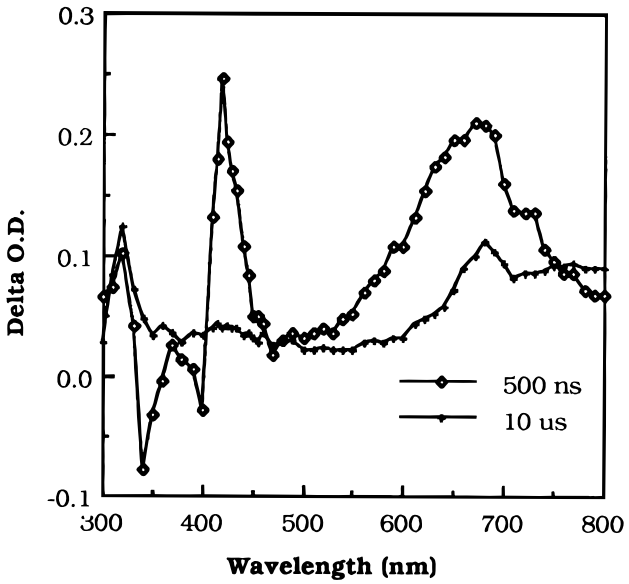

Figure 1. Transient absorption spectrum from laser flash photolysis of **1a**.

Scheme 2. Mechanism of Carbazole Formation

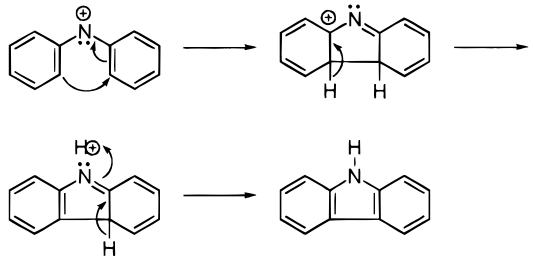

The carbazole product comes from a net rearrangement/deprotonation of Ph_2N^+. It is proposed that this occurs via a Nazarov-like electrocyclic ring closure giving intermediate **3**. The latter undergoes deprotonation followed by a proton shift to give the observed product (Scheme 2). Addition of the singlet traps CH_3OH or Cl^- suppresses the yield of this product, and it is thus assigned to the singlet manifold (Scheme 1).

The intermediacy of $Ph_2N^\bullet$ was verified by two experiments. First, it was detected by LFP. Pulsed laser photolysis (308 nm, 25−75 mJ, 10 ns) of **1a** in acetonitrile gives the transient absorption spectra shown in Figure 1. At early times there are two bands at 425 and 660 nm that are due to the singlet state of Ph_2N^+. The basis for this assignment has been presented in a previous report.[4] Following the decay of Ph_2N^+ (τ ca. 2 ms) there remain bands at 325 and 680 nm. These are due to $Ph_2NH^{+\bullet}$.[23] It is believed that the radical cation is subsequently deprotonated by 2,4,6-collidine, which is formed during photolysis (Scheme 1), thereby forming the diphenylaminyl radical, $Ph_2N^\bullet$. This intermediate has a broad absorption at 650−750 nm. The said absorption bands for $Ph_2NH^{+\bullet}$ and $Ph_2N^\bullet$ agree reasonably well with literature spectra for these species.[24−27]

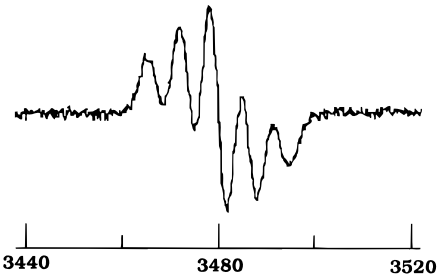

Figure 2. X-band EPR spectrum obtained from steady state irradiation of **1a** in MeCN.

Further evidence for radical chemistry was obtained from electron paramagnetic resonance spectra (EPR). When an acetonitrile solution of **1a** is irradiated in the EPR cavity under steady state conditions, an EPR spectrum is obtained (Figure 2). This spectrum contains five lines with coupling constants of 7 G. No further hyperfine splitting was observed. The small hyperfine splitting may have been lost due to the fact that a field modulation of 2.7 G was used to obtain a good signal-to-noise ratio. It is clear from the spectrum obtained that we are not observing the diphenylaminyl radical. In that case, a three-line pattern, with further hyperfine coupling due to the protons, would have been observed.[28]

It is noteworthy that the species produced from the photolysis of **1a** is extremely long lived. The EPR signal persists for several minutes after irradiation. It is possible that this species is a head-to-head dimer of a triplet nitrenium ion and DPA radical. The result of such a coupling would be the tetraphenylhydrazine radical cation. A five-line pattern similar to the one obtained from photolysis of **1a** has been observed when the radical of bis(4-methoxyphenyl)amine is generated in acetone.[28] In this case, a head-to-head dimer was proposed as the species that gives rise to the five-line EPR spectrum.

In summary, the behavior of Ph_2N^+ is in some ways reminiscent of phenylnitrene (PhN). In the absence of efficient trapping agents, both species undergo a complex series of reactions to form poorly characterized polymeric or oligomeric materials.[29] In the case of Ph_2N^+, LFP and EPR studies show that radical species are involved in these decay process. High yields of monomeric products can only be expected if high concentrations of very reactive trapping agents are present.

Addition of π-Nucleophiles to Ph_2N^+. The reactivity of the photochemically generated Ph_2N^+ ion **2** with electron rich alkenes was examined in order to determine if the simple resonance picture for nucleophile addition mentioned above suffices in explaining the regiochemistry of addition. Moreover, we wanted to see if any trends exist in C- versus N-addition as the alkene is varied. The alkenes used in this study include the silyl ketene acetals of methyl propanoate **3** and 2-methylpropanoate methyl ester **4**, the silyl enol ethers of acetone **5**, cyclohexanone **6**, and acetophenone **7**, allyltributylstannane **8**, allyltrimethylsilane **9**, and β-methylstyrene **10**. 2,3-Dihydropyran, as well as aromatic compounds, namely benzene and anisole, were also used. Most of these alkenes are shown in Figure 3.

(23) Wagner, B. D.; Ruel, G.; Lusztyk, J. *J. Am. Chem. Soc.* **1996**, *118*, 13−19.

(24) Also, a spectrum of the radical cation was generated independently by photolyzing an acetonitrile solution of DPA in the presence of dicyanobenzene (DCB) This spectrum compared favorably with those presented in the literature eventhough the 325 nm band was occluded by bands attributed to the radical anion of DCB.

(25) Shida, T.; Hamill, W. H. *J. Chem. Phys.* **1966**, *44*, 2369−2374.

(26) Scheerer, R.; Grätzel, M. *J. Am. Chem. Soc.* **1977**, *99*, 865−871.

(27) Weir, D.; Scaiano, J. C.; Schuster, D. I. *Can. J. Chem.* **1988**, *66*, 2595−2600.

(28) Nishimura, N.; Nakamura, T.; Sueishi, Y.; Yamamoto, S. *Bull. Chem. Soc. Jpn.* **1994**, *67*, 165−171.

(29) Smith, P. A. S. In *Azides and Nitrenes: Reactivity and Utility*; Scriven, E. F. V., Ed.; Academic Press: Orlando, FL, 1984; pp 95−204.

3 R_1= CH_3; R_2= OCH_3; R_3= H **8** X = $SnBu_3$
4 R_1=R_3= CH_3; R_2= OCH_3 **9** X = TMS
5 R_1=R_3= H; R_2= CH_3
6 R_1=R_2= $-CH_2CH_2CH_2-$; R_3= H;
7 R_1=R_3= H; R_2= Ph

Figure 3. Alkenes used as π-nucleophiles.

The salt **1a** from which Ph_2N^+ was generated photochemically was synthesized by the method of Balaban[30] from 1,1-diphenylhydrazine and 2,4,6-trimethylpyrrylium tetrafluoroborate. The *N*-[(4-methylphenyl)amino]pyridinium salt **1b** was synthesized in the same manner from 1,1-bis(4-methylphenyl)hydrazine.

1a reacts cleanly when it is photolyzed in the presence of 10 molar equiv of silyl ketene acetals **3** and **4**, TMS enol ethers **5**−**7**, and allyltributylstannane **8**. Only one experiment was attempted with **1b**. This experiment involved the photolysis of **1b** with **4**. The products that were isolated from all of these reactions will be described in full below. Photolyses of **1a** in the presence of allyltrimethylsilane **9**, 2,3-dihydropyran, β-methylstyrene **10**, anisole, and benzene yielded complex mixtures of products from which only Ph_2NH could be identified.

(1) Silyl Ketene Acetals. The silyl ketene acetals of propanoate methyl ester **3** and 2-methylpropanoate methyl ester **4** were used in photolyses of **1a** in acetonitrile (Scheme 3). The products that were isolated from these reactions were Ph_2NH and the corresponding para addition products **11** and **12**, as well as the corresponding 3-subtituted *N*-phenylindolinones **13** and **14** (Scheme 3). Nitrogen addition products **15** and **16** were also isolated (see Table 1).

We attribute the *N*-phenylindolinones to a mechanism involving initial ortho addition of the silyl ketene acetals to Ph_2N^+. One pathway that could lead to the formation of these compounds is illustrated in Scheme 4. This route involves initial attack of the silyl ketene acetal at the ortho position on one of the Ph_2N^+ aryl rings followed by cyclization onto the highly stabilized silyloxy carbocation. Rearomatization of the ring, followed by elimination of the elements of $TMSOCH_3$ would then yield the 3-substituted *N*-phenylindolinones **13** and **14**. The regiochemistry of the indole products argues against any alternative mechanism involving initial addition of the nucleophile to the nitrogen of Ph_2N^+. In that case we would have expected a 2-subtituted *N*-phenylisoindolinone. No such product was isolated.

An alternative mechanism for the formation of the observed indolinone products could be initial addition of the α-carbon of the silyl ketene acetal to the nitrogen of Ph_2N^+. Such an addition, however, would lead to the generation of a β-carbocation that is stabilized to a lesser extent than the α-silyloxy carbocation generated when the β-carbon of the nucleophile adds. It should also be noted that our observations do not exclude the formation of the indolinones in a concerted fashion.

In order to probe the effects of steric hinderance of the para position of the nitrenium ion **2b**, the para-substituted pyridinium salt, **1b**, was photolyzed in the presence of silyl ketene acetal **4**. As illustrated in Scheme 5, this reaction yielded bis(4-methylphenyl)amine **17** (8.1%), the

Scheme 3. Products from Photolysis of 1a in the Presence of Silyl Ketene Acetals 3 and 4 (Diphenylamine Is a Product in Both Reactions)

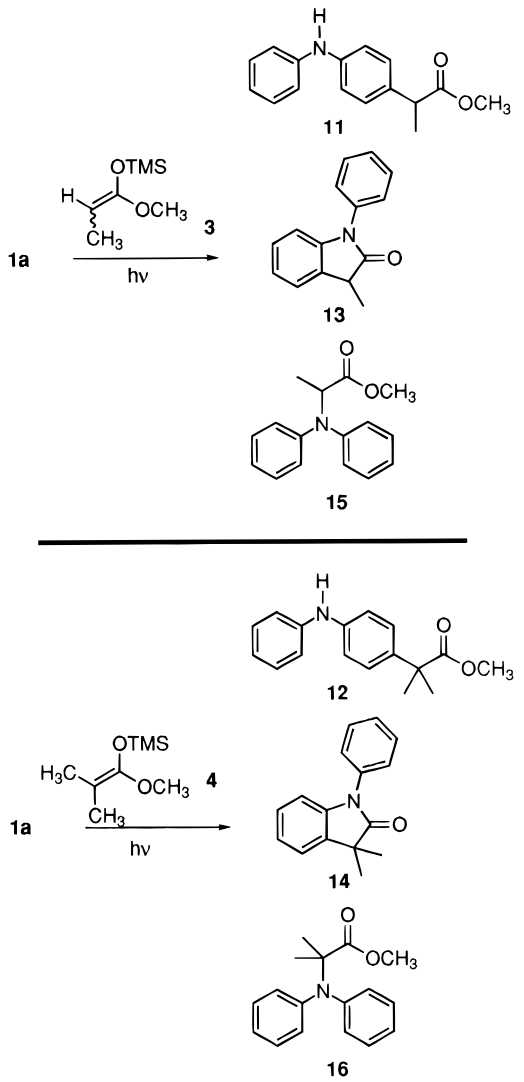

Table 1. Isolated Yields of Products from Photolyses of 1a in the Presence of 3 and 4

Nucleophile	Relative Product Yields (%)				Total Yield (%)
	Ph_2NH	Para Addition Products	N-Phenyl Indolinones	N-Addition Products	
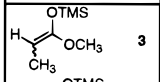 **3**	19.2	29.0 (**11**)	5.9‡ (**13**)	11.8 (**15**)	65.9
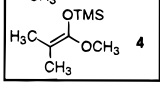 **4**	8.0	27.7 (**12**)	18.9 (**14**)	11.3 (**16**)	61.8

‡ Product Yield Determined by HPLC

nitrogen addition product **18** (25.0%), and *N*-(4-methylphenyl)-3,3,5-trimethylindolinone **19** (26.0%). What is interesting about this reaction is that the para addition product, quinone imine **20**, was isolated (15.3%) (Scheme 5). The addition product is unusual in that the silyl ketene acetal has added ipso to the methyl group of **2b**.

It is evident from the relative yields of addition products that the *p*-methyl group affects the amount of para adduct **20** that is produced. The relative ratio of combined N-addition (**16**) and cyclization product (**14**), relative to para addition product (**12**), in reactions of **1a** with **4** is 1.09. This contrasts with the results observed when **1b** is photolyzed in the presence of **4**. In this case, the ratio of the combined N-addition and cyclization

(30) Balaban, A. T.; Paraschiv, M. *Rev. Roum. Chim.* **1982**, *27*, 513−524.

Scheme 4. Mechanism for *N*-Phenylindolinone Formation

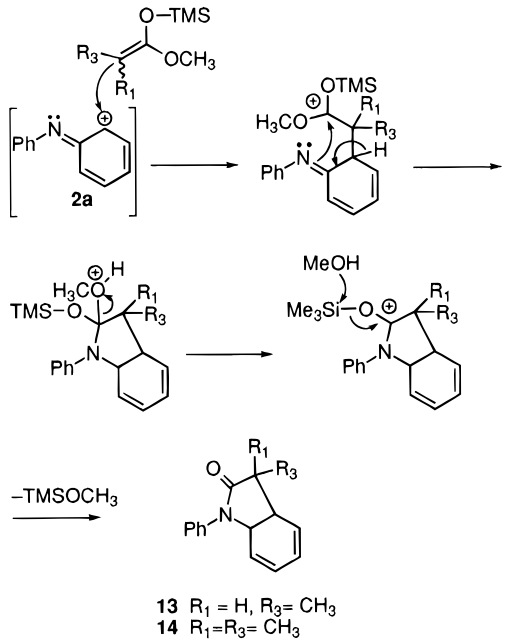

13 R_1 = H, R_3= CH_3
14 R_1=R_3= CH_3

products (**18** and **19**) relative to para addition product **20** is 3.33. A reason for such an increase is, of course, a result of steric inaccessibility of the para position due to the presence of the *p*-methyl group on **2b**.

(2) Silyl Enol Ethers. The silyl enol ethers of acetone **5**, cyclohexanone **6**, and acetophenone **7** were employed next as trapping agents for Ph_2N^+, **2a**. The products isolated from these reactions are illustrated in Scheme 6. These included Ph_2NH, the corresponding para addition products **21**−**23** and *N*-phenylindoles **24**−**26**. The isolated yields of these products are presented in Table 2. Products resulting from trapping of Ph_2N^+ at nitrogen were absent in all of these experiments. As in the case of silyl ketene acetals, the regiochemistry of the products argues against a mechanism which involves N-addition to Ph_2N^+ by the TMS enol ethers. For example, reaction of **2a** with TMS enol ethers of acetone and acetophenone lead to the 1-phenyl-2-methylindole **24** and 1,2-diphenylindole **26**, respectively. In no case are the 3-substituted *N*-phenylindoles observed.

Again, we attribute the observed indoles as resulting from initial addition to the ortho carbon giving a stabilized carbocation intermediate followed by cyclization as described above for the silyl ketene acetals. An alternative mechanism that would give the same indolinone products would involve initial addition of the alkene α-carbon to the nitrogen of Ph_2N^+. In the case of the TMS enol ethers of acetone and acetophenone, initial addition to nitrogen would be highly disfavored due to the fact that a primary carbocation would be formed. Therefore, this alternative mechanism is excluded.

(3) Reactions of 1a with Other Electron Rich Alkenes. Swenton et al. have shown that solvolysis reactions of quinone imine ketals such as **27** in the presence of acid and *β*-methylstyrene **10** formed a variety of products that are considered to be derived from a nitrenium ion (Scheme 7).[17]

The mechanism of reaction involves the nucleophilic attack of the alkene at the position ortho to the nitrenium ion nitrogen, thereby forming the stabilized benzyl carbocation. This carbocation is then trapped via two competing pathways: (i) imine cyclization to form the *N*-acyldihydroindole **28** and (ii) carbonyl cyclization to form the 7-membered cyclic imine **29**. Both **28** and **29** are produced in high yields. With this precedent in mind, we sought to determine whether similar chemistry would occur when **1a** is photolyzed in the presence of electron rich *π*-nucleophiles that do not contain the *(trimethylsilyl)oxy* moiety. These nucleophiles included allyltributyltin **8**, allyltrimethylsilane **9**, and, of course, *β*-methylstyrene **10**.

When **1a** is photolyzed in the presence of allyltributylstannane **8** (Scheme 8), the ortho and para addition products **30** and **31** were isolated, albeit in modest yields (Table 3). Isolated as well was Ph_2NH. A nucleophilic adduct that would arise from attack at nitrogen (**32**) was not detected. An *N*-phenyldihydroindole, a product analogous to Swenton's *N*-acyldihydroindole **28**, was not detected either.

The photolysis of **1a** in the presence of allyltrimethylsilane **9** did not give products attributable to the trapping of Ph_2N^+; that is, the para, ortho, and nitrogen addition products, **30**, **31**, and **32**, were not detected. Again, a product that would from cyclization of the alkene to give a product analogous to Swenton's *N*-acyldihydroindole (**28**, Scheme 7) was not detected. The only product that was isolated, in low yield, was Ph_2NH (see Table 3).

1a was photolyzed in the presence of a number of other electron rich alkenes and aromatic compounds, namely 2,3-dihydropyran, *β*-methylstyrene **10**, benzene, and anisole. In the case of photolyses run in neat benzene and anisole, triphenyl amine, and *N*,*N*-diphenyl-*N*-(4-methoxyphenyl)amine, products arising from electrophilic aromatic substitution by nitrenium ion Ph_2N^+, were expected. Such products would have been analogous to those obtained by Takeuchi when he generated H_2N^+ in the presence of such aromatic compounds.[31] However, our photolyses only yielded highly colored solutions that contained a complicated mixture of products that included Ph_2NH (determined by TLC). It is likely that in our experiments the steric demands of placing one more aryl group on an already sterically encumbered nitrenium ion disfavors the generation of triarylamines.

Photolyses of **1a** in neat 2,3-dihydropyran like photolyses in the above aromatic solvents met with little success in terms of isolable photoproducts. Photolyses of **1a** in the presence of 10 molar equiv of *β*-methylstyrene **10** in CH_3CN also failed to give the expected nucleophilic adducts. In both cases, the only product that was detected (by TLC), but not quantitated, was Ph_2NH. Even products analogous to Swenton's were not observed.

(4) Laser Flash Photolysis Studies. Three nucleophiles, 2-methylpropanoate methyl ester silyl ketene acetal **4**, cyclohexanone TMS enol ether **6**, and allyltributylstannane **8**, were studied using laser flash photolysis of **1a** in acetonitrile. Previously, we have reported that the diphenylnitenium ion **2a** is quenched by nucleophiles such as ethanol, methanol, and chloride.[4] The decay rate constants were measured with varying nucleophile concentrations. A pseudo-first-order analysis provides the second-order rate constants (k_{nuc}) of 4.9×10^6, 5.2×10^6, and 1.0×10^{10} M^{-1} s^{-1} for MeOH, EtOH, and chloride, respectively. Electron rich alkenes such as **8**, **6**, and **4** reacted with k_{nuc} of 1.1×10^9, 1.9×10^9, and 3.6×10^9 M^{-1} s^{-1}, respectively. The ordering **4** > **6** > **8** of *π*-nucleophiles in terms of their second-order rate con-

(31) Takeuchi, H.; Higuchi, D.; Adachi, T. *J. Chem. Soc., Perkin Trans. 2* **1991**, 1525−1529.
(32) Mayr, H.; Patz, M. *Angew. Chem., Int. Ed. Engl.* **1994**, *33*, 938−957.

Scheme 5. Products Resulting from the Photolysis of 1b in the Presence of 4

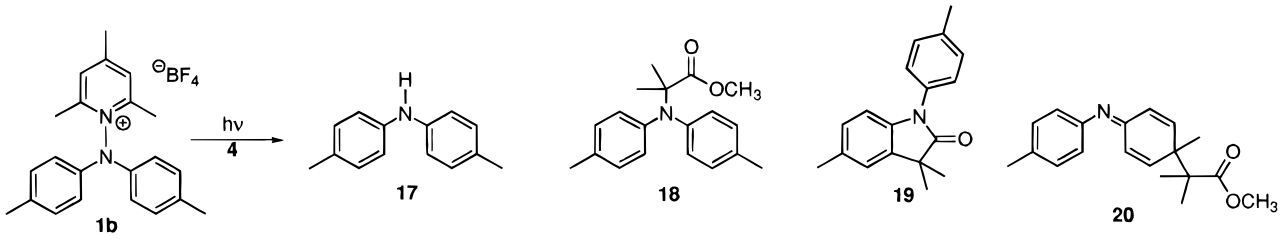

Scheme 6. Products Resulting from the Photolysis of 1a in the Presence of Silyl Enol Ethers 5−7 (Diphenylamine Is a Product in These Reactions)

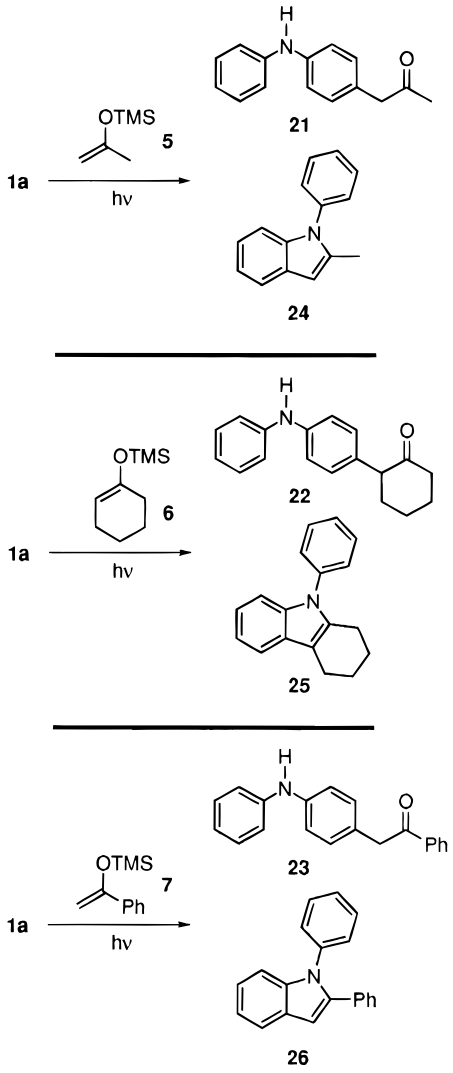

Scheme 7. Mechanism for the Formation of 28 and 29 via an *N*-acylarylnitrenium ion

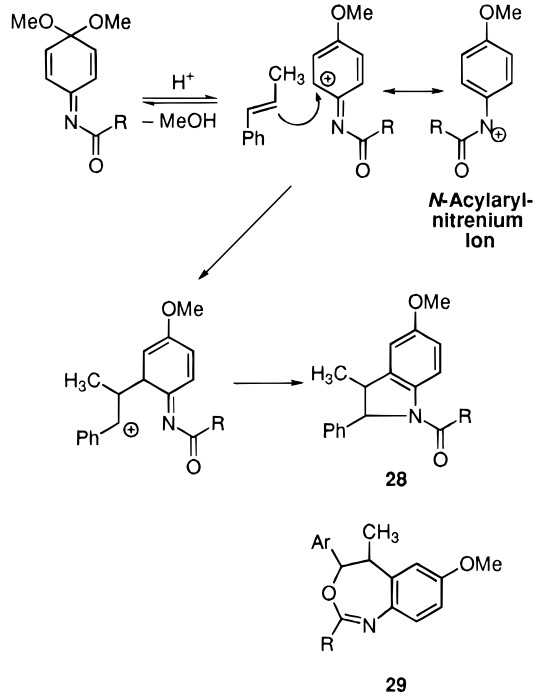

Scheme 8. Products Resulting from the Photolysis of 1b in the Presence of Allyltributylstannane 8 and Allyltrimethylsilane 9 (Diphenylamine Is a Product in This Reaction)

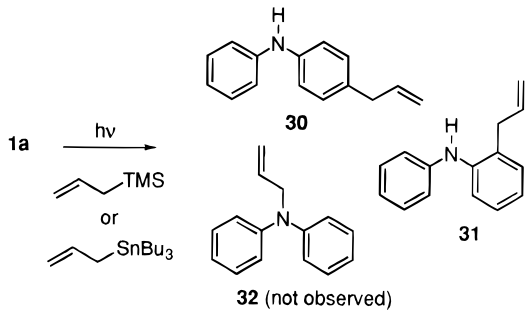

Table 2. Isolated Yields of Products from Photolyses of 1a in the Presence of 5−7

Nuclephile	Relative Product Yields (%)				Total Yield (%)
	Ph_2NH	Para Addition Products	N-Addition Products	N-Phenyl Indoles	
OTMS, CH_3 **5**	14.5	22.3 (**21**)	•	2.3 (**24**)	39.1
OTMS **6**	7.3	31.0 (**22**)	•	15.0 (**25**)	53.3
OTMS, Ph **7**	8.9	23.7 (**23**)	•	2.9 (**26**)	35.5

Table 3. Isolated Yields of Products from Photolyses of 1a in the Presence of 8 and 9

	relative product yield (%)				
nucleophile	Ph_2NH	para addition product **30**	ortho addition product **31**	N-addition product **32**	total yield (%)
allyl $SnBu_3$ **8**	7.0	16.8	12.3		36.1
allyl TMS **9**	9.6				9.6

stants has been observed for diarylcarbenium ions[32] and is therefore not surprising. For diarylcarbenium ions, the reactivity of π- nucleophiles has been correlated with their ionization potential. Similarly, we have correlated the reactivity of these selected nucleophiles with their oxidation potentials. The order of each class of alkenes in terms of decreasing oxidation potential is as follows: **4** ($E° = 0.9$ V) > **6** ($E° = 1.3$ V) > **8** ($E° \approx 1.5$ V).[33] It is

clear from these data that the more easily oxidized the alkene the faster it will react with Ph_2N^+.

(5) Molecular Orbital Analysis of Ph_2N^+. To further understand the regioselectivity in the trapping of the singlet diphenylnitrenium by different nucleophiles, we carried out a number of calculations at different levels of molecular orbital and density functional theory. Two factors that govern the regioselectivity of trapping are (i) the charge distribution in the nitrenium ion and (ii) the amplitude of the lowest unoccupied molecular orbital (LUMO) at different positions on the aromatic nitrenium ion. In the ideal limit, one might expect anionic and polarized nucleophiles to be directed entirely to the site of maximum positive charge, while electron rich, or highly delocalized π-nucleophiles would be expected to attack at the atom making the largest contribution to the LUMO (which is a π type orbital for diphenylnitrenium). Of course, actual nucleophiles will respond to each of these factors to a greater or lesser extent, as well as to other factors, like steric hinderance, local polarizability, etc. Nevertheless, the calculations provide useful details on the charge distribution and LUMO that add to the overall analysis of this phenomenon.

Calculations, which included complete geometry optimizations, were carried out at the density functional level of theory (DFT) using the gradient-corrected functionals of Becke[34] (exchange) and Perdew and Wang[35] (correlation) with the correlation-consistent polarized valence-double-ζ basis set (cc-pVDZ) of Dunning.[36] DFT is more appropriate here than more conventional molecular orbital theory because of the multideterminantal character of the nitrenium ion singlet (i.e., the wave function is best described as a linear combination of determinants the dominant one of which has the nitrogen lone pair in plane, but the one with the nitrogen lone pair conjugated with the aromatic π-system makes a nontrivial contribution). DFT has been shown to handle this multiconfigurational character efficiently and accurately both for aromatic[37] and other[37−40] nitrenium ions and for related diradical systems.[41−45] To try to identify trends, as opposed to making absolute interpretations, calculations were carried out for phenylnitrenium, diphenylnitrenium, and *N*-acetylphenylnitrenium. Experimental studies have shown relatively little tendency for phenylnitrenium to trap nucleophiles at nitrogen, while *N*-acetylphenylnitrenium and analogous compounds are well established to do so.[15] All DFT calculations were carried out with the Gaussian 94 program suite.[46]

Table 4. DFT ESP Charges q_k for $PhNH^+$, Ph_2N^+, and $PhNAc^+$

	q_k		
atom *k*	$PhNH^+$	Ph_2NH^+	$PhNAc^+$
N	−0.43	−0.45	−0.51
O			−0.42
C1	0.44	0.41	0.54
C2	0.01	−0.10	−0.05
C3	−0.12	−0.08	−0.10
C4	0.16	0.05	0.14
C5	−0.07	−0.10	−0.06
C6	−0.09	−0.10	−0.15
C7			0.80

Table 5. AM1 Atomic Contributions to LUMO for $PhNH^+$, Ph_2N^+, and $PhNAc^+$

	C_k[a]		
atom *k*	$PhNH^+$	Ph_2NH^+	$PhNAc^+$
N	0.50	0.54	0.49
O			−0.17
C1	−0.09	−0.08	−0.14
C2	−0.47	−0.34	−0.46
C3	0.00	0.02	0.02
C4	0.56	0.35	0.54
C5	0.05	0.04	0.04
C6	−0.45	−0.33	−0.44
C7			0.10

[a] See eq 4.

Chart 1

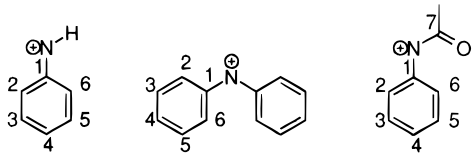

From the DFT densities, molecular electrostatic potentials were calculated. Color maps of these potentials on the 0.045 au isodensity surface are available as supporting information, where blue coloration designates areas of maximal positive potential for a positive test charge and red coloration designates areas of minimal positive potential. In addition, atomic partial charges were fit to best reproduce the electrostatic potential (ESP),[47] and those charges are listed in Table 4 (Chart 1 provides the atomic numbering scheme).

The ESP charges can be misleading to the extent that they project directional information into a single value; for instance, the molecular ESP shows clearly that the least positive region of the potential is in the vicinity of the nitrogen lone pair, which is orthogonal to the π-system, while the "empty" nitrogen lone pair is a region of high positive potential. This spatial information is not well captured in a simple atomic partial charge.

Pictures of the Kohn−Sham LUMO's for $PhNH^+$, Ph_2N^+, and $Ph(Ac)N^+$ are also available as supporting information. While not formally molecular orbitals, Kohn−Sham orbitals typically resemble closely orbitals from say, Hartree−Fock theory, and are thus useful for interpretation. One drawback of ab initio orbitals, whether from DFT or Hartree−Fock theory, is that it is

(33) Fukuzumi, S.; Fujita, M.; Otera, J.; Fujita, Y. *J. Am. Chem. Soc.* **1992**, *114*, 10271−10278.
(34) Becke, A. D. *Phys. Rev. A* **1988**, *38*, 3098−3100.
(35) Perdew, J.; Wang, Y. *Phys. Rev. B* **1992**, *45*, 13244−13249.
(36) Dunning, T. H. *J. Chem. Phys.* **1989**, *90*, 1007−1023.
(37) Cramer, C. J.; Dulles, F. J.; Falvey, D. E. *J. Am. Chem. Soc.* **1994**, *116*, 9787−9788.
(38) Cramer, C. J.; Dulles, F. J.; Storer, J. W.; Worthington, S. E. *Chem. Phys. Lett.* **1994**, *218*, 387−394.
(39) Boche, G.; Andrews, P.; Harms, K.; Marsch, M.; Rangappa, K. S.; Schimeczek, M.; Willeke, C. *J. Am. Chem. Soc.* **1996**, *118*, 4925−4930.
(40) Lim, M. H.; Worthington, S. E.; Dulles, F. J.; Cramer, C. J. *Density−Functional Methods in Chemistry*; American Chemical Society: Washington, DC, 1996; p 402.
(41) Worthington, S. E.; Cramer, C. J. To be published.
(42) Gutsev, G. L.; Ziegler, T. *J. Phys. Chem.* **1991**, *95*, 7220-.
(43) Murray, C. W.; Handy, N. C.; Amos, R. D. *J. Chem. Phys.* **1993**, *98*,
(44) Russo, N.; Sicilia, E.; Toscano, M. *Chem. Phys. Lett.* **1993**, *213*, 245−249.
(45) Smith, B. A.; Cramer, C. J. *J. Am. Chem. Soc.* **1996**, *118*, 5490−5491.
(46) Frisch, M. J.; Trucks, G. W.; Schlegel, H. B.; Gill, P. M. W.; Johnson, B. G.; Robb, M. A.; Cheeseman, J. R.; Keith, T.; Petersson, G. A.; Montgomery, J. A.; Raghavachari, K.; Al-Laham, M. A.; Zakrzewski, V. G.; Ortiz, J. V.; Foresman, J. B.; Cioslowski, J.; Stefanov, B. B.; Nanayakkara, A.; Challacombe, M.; Peng, C. Y.; Ayala, P. Y.; Chen, W.; Wong, M. W.; Andres, J. L.; Replogle, E. S.; Gomperts, R.; Martin, R. L.; Fox, D. J.; Binkley, J. S.; Defrees, D. J.; Baker, J.; Stewart, J. P.; Head-Gordon, M.; Gonzalez, C.; Pople, J. A. *Gaussian 94 Rev D. 1*; Gaussian Inc.: Pittsburgh, PA, 1995.
(47) Singh, U. C.; Kollman, P. A. *J. Comput. Chem.* **1984**, *5*, 129−145.

not easy to assign an atomic contribution to the orbital because the atomic orbital basis functions do not comprise an orthonormal set. By construction, this difficulty is removed at semiempirical levels of theory like Austin Model 1 (AM1).[48] In addition to the orbital pictures in the Supporting Information, Table 5 contains atomic contributions to the LUMO as calculated at the AM1 level of theory. These contributions, C_k, are calculated as

$$C_k = \sqrt{\sum_{i=1}^{n} c_i^2} \qquad (4)$$

where n is the number of atomic orbital basis functions found on atom k and c_i is the coefficient for basis function i in the LUMO. The sign of C_k is assigned from inspection of the phases of the orbitals. (Note that in $PhNH^+$ and $PhNAc^+$ only atomic p orbitals enter into the π LUMO; however, since Ph_2N^+ is twisted by steric interactions between the two aromatic rings, one must carry out the sum over the orbitals in eq 4.) For the most part, the AM1 LUMO's closely resemble the DFT LUMO's (as do the highest energy SOMO's from AM1 calculations on the triplet, i.e., there are no apparent difficulties associated with the AM1 orbitals being virtual), which is consistent with the qualitatively useful trends apparent in semiempirical calculations for nitrenium ions.[49−51] AM1 calculations were carried out with the AMSOL program suite at the optimized DFT geometries.[52]

Analysis of the data in Table 4 bears out the point made above that directional information is poorly captured by ESP charges. The nitrogen atoms in all three nitrenium cations have similarly large negative ESP charges because they must account for the in-plane lone pair density. The *ipso* carbon is then forced to develop a very large *positive* partial charge to help fit the low charge density associated with nitrogen in the π-system (which is easily identified in the color-mapped molecular ESP's). The para carbon atoms in each case are positively charged, which is consistent with intuition based on, say, analysis of resonance structures. However, the ortho carbons are not generally distinguishable from the meta positions, which is quite counterintuitive. Moreover, the expected polarization of the molecular ESP is clearly identifiable in the color maps in the supporting information (i.e., ortho and para positions show depleted π density relative to meta and ipso). One must conclude that ESP charges are not particularly useful for examining π-polarization. The one feature in the molecular ESP's that *does* show up in the ESP charges, albeit in a hidden way, is the very large area of depleted density surrounding the nitrogen atom in $PhNAc^+$. In the ESP charges, this is identifiable in the extremely large positive charges for the ipso carbon (0.54) and the carbonyl carbon (0.80). It may well be that this "sea" of depleted electronic charge density, which is not observed for either $PhNH^+$ or Ph_2N^+, is responsible for guiding in nucleophiles to attack nitrogen in $PhNAc^+$, consistent with the experimental observations for greater N-substitution with this substrate.

The atomic LUMO coefficients in Table 5 provide some additional interesting information. For instance, in all three nitrenium ions there is essentially no contribution to the LUMO from the meta carbon atoms, which is consistent with the absence of meta substitution for these substrates (note that this analysis is distinct and complementary to charge polarization). As for comparisons of N, ortho, and para coefficients, in $PhNH^+$ and $PhNAc^+$, there is very little difference in magnitude across these positions—this is entirely consistent with the DFT orbital visualizations as well (see Supporting Information). In Ph_2N^+, on the other hand, the N coefficient is about 50% larger than the ortho and para coefficients. However, the DFT orbital visualizations show similar amplitudes on all three positions, suggesting that the AM1 results may be an artifact. Thus, it does not seem that regioselectivity in the trapping of nucleophiles by these nitrenium ions is strongly directed by differential amplitudes in the LUMO, except to the extent that in every case the near-zero amplitude of the LUMO at the meta positions reinforces the charge polarization and makes this position very unattractive to incoming nucleophiles.

In summary, for $PhNH^+$ and Ph_2N^+, there do not seem to be effects associated with either the charge distribution or the LUMO that would strongly influence ortho/para/N selectivity in nucleophilic trapping. To the extent that any influences *are* present, they are almost certainly no larger than steric influences or possible solvation effects, etc. In $PhNAc^+$, there *is* a noticeable decrease in electronic charge density over the nitrogen atom which may be responsible for the much greater tendency of this substrate to undergo nucleophilic substitution at nitrogen in experimental systems.

Conclusions

It is clear that a*b initio* and semiempirical calculations on isolated nitrenium ions do not provide obvious indications that would allow one to predict the preferred site of addition of nucleophiles. In most cases, the major trapping product isolated experimentally is the para addition product. The ortho addtion product is always produced in smaller yields. Addition to nitrogen occurs in low yields and only when silyl ketene acetals were used as nucleophiles. These data clearly indicate a bias for reaction at the para position on the aromatic ring; this is not borne out in the FMO analysis of Ph_2N^+. A more careful theoretical analysis which includes locating transition states for nucleophilic addition may be of greater predictive value. However, that is beyond the scope of the present study.

One clear correlation that can be found, however, is in the oxidation potentials of the alkenes and their second-order rate constants; that is, the lower the oxidation potential the faster the rate of addition to Ph_2N^+. A similar trend has been found in reactions of carbenium ions with alkenes.[53,54] Moreover, by comparing the second-order nucleophilic constants of n-nucleophiles with those of π-nucleophiles, it becomes evident that as the diffusion limit is approached, the selectivity of addition is lost. So, for example, the n-nucleophile MeOH, which has a relatively modest second-order rate constant ($k_{nuc} = 5.2 \times 10^6\ M^{-1}\ s^{-1}$), adds only at the para

(48) Dewar, M. J. S.; Zoebisch, E. G.; Healy, E. F.; Stewart, J. J. P. *J. Am. Chem. Soc.* **1985**, *107*, 3902−3909.
(49) Ford, G. P.; Scribner, J. D. *J. Am. Chem. Soc.* **1981**, *103*, 4281−4291.
(50) Glover, S. A.; Scott, A. P. *Tetrahedron* **1989**, *45*, 1763−1776.
(51) Falvey, D. E.; Cramer, C. J. *Tetrahedron Lett.* **1992**, *33*, 1705−1708.
(52) Hawkins, G. D.; Lynch, G. C.; Giesen, D. J.; Rossi, I.; Storer, J. W.; Liotard, D. A.; Cramer, C.; Truhlar, D. G. *QCPE Bull.* **1996**, *16*, 11.
(53) Mayr, H. *Angew. Chem., Int. Ed. Engl.* **1990**, *29*, 1371−1522.
(54) Bartl, J.; Steenken, S.; Mayr, H. *J. Am. Chem. Soc.* **1991**, *113*, 7710−7716.

position of **2a**. In the case of very reactive π-nucleophiles, such as silyl ketene acetal **4** ($k_{nuc} = 3.6 \times 10^9$ M^{-1} s^{-1}), selectivity decreases; not only is para and ortho addition observed, but N-addition as well. Similarly, chloride ($k_{nuc} = 1.0 \times 10^{10}$ M^{-1} s^{-1}) adds at both the para and ortho positions of **2a**.[4]

Experimental Section

General. ^1H and ^{13}C NMR spectra were recorded on a Bruker AF200 spectrometer (200.132 MHz ^1H, 50.32 MHz ^{13}C). Some selected ^1HNMR spectra were recorded on a Bruker AM 400 (400.132 MHz ^1H). EtOAC and hexane were distilled prior to use. CH_3CN was distilled from CaH_2 through a vacuum-sealed column (30 cm) packed with glass helices. CH_2Cl_2 was distilled from CaH_2. HPLC was performed on a Rainin Gradient HPLC system with a variable wavelength detector (Linear UVIS 200) set at 254 nm. Analytical work was performed with a microsorb-MV 5 μm C-18 column from Rainin. The solvent system in all cases was a H_2O/CH_3CN mixture. The flow rate was, in all cases 1 mL/min. Thin layer chromatography (TLC) was performed on precoated 0.25 mm glass-backed plates. Silica coating contained a fluorescent indicator, and the compounds were identified using a UV shortwave (254 nm) lamp, iodine, vanillin stain, or phosphomolybdic acid stain. Chromatography was performed using a Harrison research radial chromatotron (Model 7924T) or by standard flash chromatography methods. The silica gel used in each flash column chromatography run was Davisil gel (grade 633, 200−425 mesh, 60 Å average particle size). Mass spectral results (MS) are reported as m/z values and are EI unless otherwise stated. Melting points are corrected. Laser flash photolysis experiments were performed using a Questek series 2100 XeCl excimer laser (308 nm, 10 ns pulse, 60−80 mJ output). Steady state photolyses where performed in a Rayonet photoreactor using fluorescent bulbs (350 nm). All photolyses were performed in Pyrex round bottom flasks unless otherwise stated. All solutions were purged with dry nitrogen for at least 10 min prior to photolysis and LFP.

Synthesis of Pyridinium Salts 1a and 1b. *N*-(Diphenylamino)-2,4,6-trimethylpyridinium Tetrafluoroborate (1a).[30] 1,1-Diphenylhydrazine (2.00 g, 0.0108 mol) was dissolved in 25 mL of EtOH. The hydrazine solution was added to a stirred solution of 2,4,6-trimethylpyrylium tetrafluoroborate (2.16 g, 0.0103 mol) in 25 mL of EtOH. The reaction was refluxed for 1 h. The resulting reaction mixture was allowed to cool to room temperature. The solution was placed in the freezer for 1 h. After this time the product precipitated out of solution as yellow plates. The crystals were filtered and washed with copious amounts of 95% EtOH, followed by Et_2O (25 mL). The crystals were dried *in vacuo* and weighed (3.15 g, 81%). **1a** proved to be pure by NMR and was not purified further: mp 165−167 °C dec; ^1H NMR ($CDCl_3$) δ 7.89 (s, 2H), 7.40 (m, 4H), 7.17 (m, 4H), 6.90 (m, 2H), 2.70 (s, 3H), 2.58 (s, 6H); ^{13}C ($CDCl_3$) δ 162.3, 157.8, 139.9, 130.8, 130.6, 125.2, 117.4, 22.5, 20.1; UV−vis (CH_3CN) 269, 373 nm.

***N*-[Bis(4-methylphenyl)amino]-2,4,6-trimethylpyridinium Tetrafluoroborate (1b).** 1,1-(Bis(4-methylphenyl)hydrazine (0.165 g, 0.7 mmol) was dissolved in 6 mL of EtOH. The hydrazine was added to a well-stirred solution of 2,4,6-trimethylpyrylium tetrafluoroborate (0.163 g, 0.7 mmol) dissolved in 3 mL of EtOH. The reaction mixture was refluxed for 30 min. At the end of the reflux period the reaction was allowed to cool to room temperature. Et_2O (5 mL) was added to the reaction mixture prior to being placed in the freezer. After 1 h in the freezer, microcrystals precipitated out of solution. The crystals were washed first with cold EtOH followed by water and then Et_2O. The bright yellow microcrystals were subsequently dried in vacuo and weighed (0.187 g, 59%): mp 151−153 °C; ^1H NMR (CD_3CN) δ 7.75 (s, 2H), 7.20 (d, 9.5 Hz, 4H), 6.83 (d, 9.5 Hz, 4H), 2.61 (s, 3H), 2.48 (s, 6H), 2.31 (s, 6H); ^{13}C; UV−vis (CH_3CN) 270, 390 nm.

Photolysis of 1a in the Absence of Traps. A solution of 139.8 mg (0.372 mmol) of **1a** in 80 mL of CH_3CN was prepared. The solution was purged for 10 min with N_2. A 20 mL aliquot of this stock solution was placed in a round bottom flask and phololyzed for exactly 1 h. A 50 μL aliquot of the photolysate was injected into the HPLC. The solvent mixture used in this experiment was 65:35 acetonitrile/water. A number of peaks were obtained, two of which could be unequivocally identified. A peak with retention time 7.61 min was assigned to carbazole. Another peak with retention time 9.21 min was assigned to Ph_2NH.

Photolysis of 1a in the Presence of π-nucleophiles. General Procedure: Illustrated with Allyltrimethylsilane (9). 1a (0.200 g, 0.53 mmol) was dissolved in 20 mL of CH_3CN in a Pyrex flask. Allyl TMS (0.84 mL, 0.6 g, 5.3 mmol) was added via syringe. The solution was purged with nitrogen prior to photolysis. The solution was photolyzed for 1 h. Following photolysis, the solvent was removed in vacuo to reveal a dark green oil. The oil was taken up in 20 mL of CH_2Cl_2. Silica gel (1 g) was added to this solution. The CH_2Cl_2 was removed. The dried silica gel was loaded onto a flash column (30 cm × 20 mm) that had been packed with 20 cm of silica gel. The column was first eluted with 200 mL of a 10:1 hexane/EtOAc solvent mixture, followed by 200 mL of a 3:1 hexane/EtOAc solvent mixture. Ph_2NH (8.6 mg) and carbazole (2.6 mg) were the only compounds isolated. Their combined yield was 12.5%.

Allyltributyltin (8). 1a (0.201 g, 0.53 mmol) was dissolved in 20 mL of CH_2Cl_2. Allyl $SnBu_3$ (1.6 mL, 1.71 g, 5.1 mmol) was added. The solution was purged with N_2 for 10 min and then photolyzed for 1 h. The solvent was removed, and the product mixture was subjected to flash column chromatography. Ph_2N (6.3 mg), para addition product **30** (18.8 mg), and ortho addition product **31** (13.8 mg) were isolated. The overall isolated yields of combined photolysis products was 36.4%. **30**: ^1H NMR ($CDCl_3$) δ 7.29−7.21 (m, 3H), 7.12−7.01 (m, 5H), 6.93−6.86 (m, 2H), 6.07−5.87 (m, 1H), 5.64 (br s, 1H, N−H), 5.12−5.03 (m, 2H), 3.36−3.32 (m, 2H); ^{13}C ($CDCl_3$) δ 143.7, 141.1, 137.8, 133.0, 129.4, 129.3, 120.6, 118.6, 117.2, 115.5, 39.5; HRMS calcd for $C_{15}H_{15}N$ 209.1204, found 209.1199. **31**: ^1H NMR ($CDCl_3$) δ 7.32−7.17 (m, 5H), 7.00−6.88 (m, 4H), 6.09−5.89 (m, 1H), 6.89 (m, 1H), 5.63 (br s, 1H, N−H), 5.19−5.04 (m, 2H), 3.41−3.37 (m, 2H); ^{13}C ($CDCl_3$) δ 144.0, 141.5, 136.4, 130.6, 129.6, 129.3, 127.3, 122.1, 120.3, 119.3, 117.2, 116.2, 36.7; HRMS calculated for $C_{15}H_{15}N$ 209.1204, found 209.1207.

2-[(Trimethylsilyl)oxy]propene (5). This reaction was run in the same manner as the reaction of **1a** with **9**. The amount of **1a** and **5** used in this case was 0.200 g (0.531 mmol) and 1.2 mL (0.943 g, 7.24 mmol), respectively. The resulting oil was dry loaded onto a column and subjected to flash column chromatography, eluting with 200 mL of 10:1 hexane/EtOAc, followed by 100 mL of 5:1 hexane/EtOAc, and finally with 100 mL of 3:1 hexane/EtOAc. The products obtained were Ph_2NH (13.3.mg), *N*-phenylindole **24**[55] (2.6 mg) and para addition product **21** (27.2 mg). The overall yield of this reaction was 39.1%. **21**: ^1H NMR ($CDCl_3$) δ 7.35−7.22 (m, 3H), 7.10−6.88 (m, 6H), 5.75 (br s, 1H, N−H), 3.62 (s, 2H), 2.15 (s, 3H); ^{13}C ($CDCl_3$) δ 206.8, 143.0, 142.2, 130.3, 129.3, 126.5, 121.0, 118.0, 117.9, 50.2, 29.1; HRMS (FAB) calculated for $C_{15}H_{16}NO$ 226.1232, found 226.1221.

1-[(Trimethylsilyl)oxy]-1-cyclohexene (6). The amount of **1a** and **6** used in this case was 0.191 g (0.507 mmol) and 1.0 mL (0.87 g, 5.13 mmol), respectively. Ph_2NH (6.3 mg), *N*-phenyltetrahydrocarbazole **25**, and para addition product **22** (18.9 mg) were obtained following column chromatography (4:1 hexane/CH_2Cl_2). The overall yield for this reaction was 53.3%. **25**: ^1H NMR ($CDCl_3$) δ 7.54−7.34 (m, 6H), 7.24−7.08 (m, 3H) 1.92−1.86 (m, 4H); ^{13}C ($CDCl_3$) δ 138.1, 137.2, 135.8, 129.3, 127.8, 127.2, 127.0, 121.3, 119.6, 117.7, 111.0, 109.8, 23.4, 23.2, 23.1, 21.1; DEPT ($CDCl_3$, 400 MHz) peaks at 23.4, 23.2, 23.1, 21.1 are all CH_2; HRMS calculated for $C_{18}H_{17}N$ 247.1361, found 247.1368. **22**: recrystallized from EtOH, mp 134−136 °C; ^1H NMR ($CDCl_3$) δ 7.27−7.19 (m, 2H), 7.05−7.01 (m, 6H), 6.92−6.85 (m, 1H), 5.75 (br s, 1H, N−H), 3.53 (m, 1H), 2.49−1.79 (m, 8H); ^{13}C ($CDCl_3$) δ 210.6, 143.3, 141.8, 131.2, 129.2, 120.6, 117.8, 117.6, 56.6, 42.1, 35.1, 27.8, 25.2; HRMS calculated for $C_{18}H_{19}NO$ 265.1464, found 265.1468.

(55) Bowman, W. R.; Westlake, P. J. *Tetrahedron* **1992**, *48*, 4027−4038.

1-Phenyl-1-[(trimethylsilyl)oxy]ethylene (7). The amount of **1a** and **7** used in this case was 0.205 g (0.546 mmol) and 1.15 mL (1.07 g, 5.60 mmol), respectively. The para addition product **23** (4.2 mg) was obtained cleanly following column chromatography (10:1 hexane/EtOAc). The other two products, Ph_2NH and *N*-phenylindole **26**, were isolated together. After a second round of chromatography using 4:1 hexane/CH_2Cl_2, Ph_2NH (8.3 mg) and **26** (4.2 mg) were obtained cleanly. The overall yield for this reaction was 35.5%: **23**: recrystallized from EtOH, mp 122−123 °C; ^{1}H NMR ($CDCl_3$) δ 8.03−7.99 (m, 2H), 7.54−7.40 (m, 3H), 7.27−6.89 (m, 9H), 5.71 (br s, 1H, N−H), 4.20 (s, 2H); ^{13}C ($CDCl_3$) δ 197.9, 143.1, 141.9, 136.6, 133.0, 130.3, 129.2, 128.5, 126.7, 120.8, 117.9, 117.7, 44.7; HRMS (FAB) calculated for $C_{20}H_{18}NO$ 288.1388, found 288.1389.

1-Methoxy-1-[(trimethylsilyl)oxy]propene (3). The amount of **1a** and **3** used in this case was 0.206 g (0.549 mmol) and 0.905 g (5.64 mmol), respectively. Ph_2NH (19.2 mg), N-addition product **15** (11.8 mg), and para addition product **11** (39.0 mg) were obtained cleanly following two rounds of column chromatography (5:1 hexane/EtOAc, followed by 4:1 hexane/CH_2Cl_2). In the first round, Ph_2NH and **15** were isolated as a mixture, separate from **11** and *N*-phenylindolinone **13**; **11** and **13** were isolated together (confirmed by ^{1}H NMR, HPLC, and GCMS results). The mixture of Ph_2NH and **15** was separated in the second round. The mixture of **11** and **13** was injected into the HPLC (20 mL, 70:30 CH_3CN/water). Using a concentration curve constructed using a sample of *N*-phenylindolinone **13** synthesized by an alternate route,[56] a mass of 5.9 mg was extrapolated. The mixture of **11** and **13** was then chromatographed (4:1 hexane/CH_2Cl_2). Only the para addition product **11** was isolated. The overall yield for this reaction was 61.8%. **11**: ^{1}H NMR ($CDCl_3$) δ 7.28−7.20 (m, 4H), 7.06−6.94 (m, 4H), 6.20−6,88 (m, 1H), 5.74 (br s, 1H, N−H), 3.67 (q, 1H), 3.65 (s, 3H), 1.47 (d, 3H); ^{13}C ($CDCl_3$) δ 175.5, 143.1, 142.2, 132.9, 129.3, 128.3, 120.9, 117.9, 117.8, 51.9, 44.7, 18.5; HRMS calculated for $C_{16}H_{17}NO_2$ 255.1259, found 255.1250. **15**: ^{1}H NMR ($CDCl_3$) δ 7.24−7.17 (m, 4H), 6.97−6.84 (m, 6H), 4.63 (q, 1H), 3.67 (s, 3H), 1.32 (d, 3H); ^{13}C ($CDCl_3$) δ 174.5, 146.1, 129.2, 122.4, 122.2, 57.2, 52.1, 16.8; HRMS calculated for $C_{16}H_{17}NO_2$ 255.1259, found 255.1261. **13** (synthetic): ^{1}H NMR ($CDCl_3$) δ 7.55−7.04 (m, 8H), 6.80 (m, 1H), 3.61 (q, 1H), 1.58 (d, 3H); ^{13}C ($CDCl_3$) δ 177.8, 143.8, 134.5, 130.3, 129.4, 127.8, 127.6, 126.4, 123.6, 122.7, 109.1, 53.3, 40.6, 15.5.

1-Methoxy-1-[(trimethylsilyl)oxy]-2-methylpropene (4). Reaction with 1a. The amount of **1a** and **4** used in this case was 0.202 g (0.537 mmol) and 0.935 g (5.37 mmol), respectively. Ph_2NH (7.3 mg), N-addition product **16** (11.8 mg), para addition product **12** (40.4 mg), and *N*-phenylindolinone **14** (24.3 mg) were obtained cleanly following two rounds of column chromatography (5:1 hexane/EtOAc followed by 4:1 hexane/CH_2Cl_2). In the first round, Ph_2NH and N-addition product **16** were isolated as a mixture, separate from the para addition product **12** and *N*-phenylindolinone **14**; **12** and **14** were isolated together. Both mixtures were separated in the second round. The overall yield for this reaction was 65.9%. **12**: ^{1}H NMR ($CDCl_3$) δ 7.28−7.20 (m, 4H), 7.06−6.98 (m, 4H), 6.94−6.87 (m, 1H), 5.71 (br s, 1H, N−H), 3.64 (s, 3H), 1.56 (s, 6H); ^{13}C ($CDCl_3$) δ 177.4, 143.1, 141.7, 137.0, 129.2, 126.5, 120.9, 117.8, 117.5, 52.1, 45.8, 26.5; HRMS calculated for $C_{17}H_{19}NO_2$ 269.1416, found 269.1412. **16**: ^{1}H NMR ($CDCl_3$) δ 7.29−7.21 (m, 4H), 7.03−6.96 (m, 2H), 6.83−6.79 (m, 4H) 3.75 (s, 3H), 1.48 (s, 6H); ^{13}C ($CDCl_3$) δ 177.8, 146.0, 128.9, 123.8, 122.1, 61.5 52.6, 26.4; HRMS calculated for $C_{17}H_{19}NO_2$ 269.1416, found 269.1409. **14**: ^{1}H NMR ($CDCl_3$, 400 MHz) δ 7.55−7.51 (m, 2H), 7.44−7.40 (m, 3H), 7.29−7.28 (m, 1H), 7.20−7.17 (m, 1H), 7.12−7.10 (m, 1H), 6.87−6.85 (m, 1H), 1.50 (s, 6H); ^{13}C ($CDCl_3$, 400 MHz) δ 180.7, 142.9, 135.6, 134.6, 129.5, 127.8, 127.5, 126.5, 122.9, 122.6, 109.3, 44.3, 24.7; HRMS calculated for $C_{16}H_{15}NO$ 237.1154, found 237.1147.

Reaction with 1b. The amount of **1b** and **4** used in this case was 0.168 g (0.416 mmol) and 0.810 g (4.64 mmol), respectively. Bis(4-methylphenyl)amine **17**[57] (6.5 mg), N-addition product **18** (30.9 mg), *N*-(4-methylphenyl) quinone imine/para addition product **20** (18.9 mg), and *N*-(*p*-tolyl)-3,3,5-trimethylindolinone **19** (28.7 mg) were obtained cleanly following two rounds of column chromatography (5:1 hexane/EtOAc followed by 4:1 hexane/CH_2Cl_2). In the first round, **17** and **18** were isolated as a mixture, separate from **19** and **20**; **19** and **20** were isolated together. Both mixtures were separated in the second round. The overall yield for this reaction was 74.4%. **17**: ^{1}H NMR ($CDCl_3$) δ 7.06 (d, 8.2 Hz, 4H), 6.94 (d, 8.2 Hz, 2H), 5.50 (br s, 1H, N−H), 2.29 (s, 6H). **18**: ^{1}H NMR ($CDCl_3$) δ 7.03 (d, 8.2 Hz, 4H), 6.71 (d, 8.2 Hz, 4H), 3.74 (s, 3H), 2.29 (s, 6H), 1.46 (s, 6H); ^{13}C ($CDCl_3$) δ 178.0, 143.8, 131.4, 129.5, 123.7, 61.4, 52.5, 26.3, 20.6; HRMS calculated for $C_{19}H_{23}NO_2$ 297.1729, found 297.1726. **19**: ^{1}H NMR ($CDCl_3$) δ 7.29 (m, 4H), 7.08 (s, 1H), 6.97 (d, 8.0 Hz, 2H), 6.71 (d, 8.0 Hz, 2H), 2.40 (s, 3H), 2.35 (s, 3H), 1.46 (s, 6H); ^{13}C ($CDCl_3$) δ 180.7, 140.3, 137.5 135.7, 132.3, 132.2, 130.1, 130.0, 127.7, 126.2, 123.3, 109.1, 44.3, 24.7, 21.1, 21.0; HRMS calculated for $C_{18}H_{19}NO$ 265.1467, found 265.1456. **20**: ^{1}H NMR ($CDCl_3$) δ 7.11 (d, 8.0 Hz, 2H), 6.73 (d, 8.0 Hz, 2H), 6.48 (m, 2H), 6.36 (m, 2H), 3.69 (s, 3H), 2.33 (s, 3H), 1.21 (m, 6H); ^{13}C ($CDCl_3$) δ 175.9, 156.8, 147.8, 145.5, 143.4, 133.1, 129.9, 129.3, 120.6, 120.3, 51.7, 48.9, 44.8, 22.2, 21.8, 21.7, 20.8; HRMS calculated for $C_{19}H_{23}NO_2$ 297.1729, found 297.1724.

EPR Spectrum from Photolysis of 1a in CH_3CN. 1a (20 mg, 0.053 mmol) was dissolved in CH_3CN (10 mL). The solution was purged for 10 min. with N_2. A 0.4 mL aliquot of this solution was transferred to an EPR tube that had been purged with N_2. The sample was placed in the EPR cavity, and a background spectrum was taken. As expected, no EPR spectrum was obtained. The sample was then irradiated for 2 min with a medium-pressure Hg lamp. The spectrum was scanned at X-band. The modulation amplitude and frequency were 2.683 G and 100 kHz, respectively. A signal was observed at 3480 G. The signal was split into a five-line pattern with 7 G coupling and no further hyperfine coupling. A spectrum was simulated using an a_N value of 6.0 obtained from the literature[28] and a line broadening of 2.9 G. The spectrum thus generated was identical to the experimental spectrum.

Laser Flash Photolysis (LFP) Experiments with 4, 6, and 8. In all cases 60 mg (0.159 mmol) of **1a** was dissolved in 60 mL of CH_3CN in a flow cell equipped with a magnetic stirrer. The solution was purged with dry N_2 for 10 min. The nucleophile was added neat, via microliter syringe in all cases. The nucleophile concentration range over which kinetic data were collected for alkenes **4**, **6**, and **8** was $0-5.6 \times 10^{-3}$, $0-4.3 \times 10^{-3}$, and $0-3.2 \times 10^{-3}$ M, respectively. The wavelength at which data was collected was 425 nm. The decay waveforms obtained in these experiments were fitted using a pseudo-first-order decay function. The values for the pseudo-first-order rate constants thus obtained were then plotted versus increasing concentration for each nucleophile. The second-order rate constant was obtained from the linear least-squares fit of these data.

Acknowledgment. The authors thank the NSF for their generous support of this work.

Supporting Information Available: ^{1}H and ^{13}C NMR spectra of the compounds characterized in this study (33 pages). Color maps of the molecular electrostatic potentials obtained from the DFT densities and pictures of Kohn-Sham LUMO's for $PhNH^+$, Ph_2N^+, and $Ph(Ac)N^+$ are available electronically. This material is contained in libraries on microfiche, immediately follows this article in the microfilm version of the jounal, and can be ordered from the ACS; see any current masthead page for ordering information.

JO9623649

(56) Rodriguez, A. C.; Leeming, P. R. *J. Med. Chem.* **1972**, *15*, 762−770.

(57) Barton, D. H. R.; Donnelly, D. M. X.; Finet, J.-P.; Guiry, P. J. *J. Chem. Soc., Perkin Trans. 1* **1991**, *9*, 2095−2102.